

Feedback Gain Design Method for the Full-Order Flux Observer in Sensorless Control of Induction Motor

Abderrahmane Bouhenna, Abdellah Mansouri, Mohammed Chenafa, Abdelkader Belaidi

Abstract: This paper deals with a feedback gain design method for the full-order flux observer with adaptive speed loop, which enables the minimizing the unstable operation region of this observer to a line in the torque-speed plane. The stability in regenerating mode is studied using necessary condition of stability based on determinant of matrix and a linearized model. Simulations results where the proposed observer is compared with an exiting solution (where the unstable region is not totally removed) are presented to validate the proposed observer design.

Keywords: Induction motor, full-order flux observer, sensorless control, stability analysis, adaptive speed estimator, regenerating mode

1 Introduction

The speed-sensorless control of induction motor drives have developed significantly during the last number of years. Speed adaptive full observers introduced by [8], [15] are promising flux estimators for inductions motors drives. The speed adaptive observer consists of a state variable observer augmented with a speed adaptation loop. The observer gain and the speed adaptive law determine the properties of the observer. The speed adaptation law is based on the component of the current estimation error with the estimated rotor flux. The adaptation law was originally derived using the Lyapunov stability theory [8]. However, the stability of the adaptation law is not guaranteed and stability problem exist in the regenerating mode. The derivation in [8] neglects a term including the actual rotor flux (which is not measurable). The positive-realness condition is not satisfied as shown [5]. Some limits of operation were quickly highlighted [9], [13]. In particular, a well known instability region was described in regenerating mode. Thus, the drive stability can't be guaranteed when this type of observer is associated with a field oriented control. There was many work in order to reduce this region of instability which is due to inadequate observer design [1, 2, 5, 14]. In this paper, we describe the design of an adaptation law that minimizes the instability region of an adaptive speed estimator. The paper is organized as follows. The induction motor model and the speed adaptive flux observer are first defined in section 2 and 3 respectively. We introduce the observer gain design in section 4 leading to a reduced instability region limited to a line. Finally, simulations results are presented and discussed in section 5, where the proposed observer is compared with an exiting solution [5, 13].

2 Induction motor model

The induction motor is described by the following state equations in the synchronous rotating reference frame with complex notations:

$$\frac{d}{dt}\underline{x} = \underline{A}(\omega, \omega_s)\underline{x} + \underline{B}\underline{u}_s \quad (1)$$

$$\underline{i}_s = \underline{C}\underline{x} \quad (2)$$

where $\underline{x} = [\underline{\psi}_r \quad \underline{i}_s]^T$

$$\underline{A} = \begin{bmatrix} -(\frac{1}{T_r} + j\omega_{sl}) & \frac{L_m}{T_r} \\ \frac{L_m}{b}(\frac{1}{T_r} - j\omega) & -(a + j\omega_s) \end{bmatrix}, \underline{B} = \begin{bmatrix} 0 \\ 1 \\ \sigma L_s \end{bmatrix}, \underline{C} = [\underline{0}_{(2 \times 2)} \quad \underline{I}], \underline{I} = \begin{bmatrix} 1 & 0 \\ 0 & 1 \end{bmatrix} \quad (3)$$

and the mechanical equation is:

$$\frac{d}{dt}\omega = p^2 \frac{L_m}{JL_r} \Im(i_s \underline{\psi}_r^*) - p \frac{T_L}{J} \quad (4)$$

where $*$ means a conjugate, j a complex number and \Im an imaginary part. $\underline{\psi}_r$: rotor flux; i_s : stator current; \underline{u}_s : stator voltage; ω_s : stator angular frequency; ω : motor angular speed; $\omega_{sl} = \omega_s - \omega$: slip angular frequency; R_s, R_r : stator and rotor resistance; L_s, L_r : stator and rotor self-inductance; L_m : mutual inductance; T_L : load torque; J : rotor inertia; p : number of pole pairs; $T_r = L_r/R_r$: rotor time constant; $a = (L_r^2 R_s + L_m^2 R_r)/(\sigma L_s L_r^2)$; $b = \sigma L_s L_r$; $\sigma = 1 - (L_m^2)/(L_s L_r)$: leakage coefficient.

3 Adaptive Observer

The conventional full-order observer, which estimates the stator current and the rotor flux together [10, 11], is written as the following state equation.

$$\frac{d}{dt}\hat{\underline{x}} = \hat{\underline{A}}(\hat{\omega}, \hat{\omega}_s)\hat{\underline{x}} + \underline{B}\underline{u}_s + \underline{G}(i_s - \hat{i}_s) \quad (5)$$

$$\hat{i}_s = \underline{C}\hat{\underline{x}} \quad (6)$$

where $\hat{\cdot}$ means the estimated values and $\underline{G} = [\underline{G}_1 \quad \underline{G}_2]^T$ is the observer gain matrix.

We assume that all machine parameters are perfectly known except the motor speed. Using the assumption of constant angular rotor speed $\dot{\omega} = 0$ (i.e. the speed variations are slow with respect to electrical mode) [8], [5], the speed adaptive law is [8]:

$$\frac{d}{dt}\hat{\omega} = \frac{\lambda L_m}{b} (e_{id}\hat{\psi}_{rq} - e_{iq}\hat{\psi}_{rd}) \quad (7)$$

where λ is a positive constant and will be tuned in (7) to improve observer dynamics. In practice, proportional-integral action is used in order to improve the dynamic behavior of the estimator.

$$\frac{d}{dt}\hat{\omega} = K_p \frac{d}{dt}(e_{id}\hat{\psi}_{rq} - e_{iq}\hat{\psi}_{rd}) + K_i(e_{id}\hat{\psi}_{rq} - e_{iq}\hat{\psi}_{rd}) \quad (8)$$

where $e_{id} = i_{sd} - \hat{i}_{sd}$, $e_{iq} = i_{sq} - \hat{i}_{sq}$, (i_{sd}, i_{sq}) are (d,q) components of stator current, (ψ_{rd}, ψ_{rq}) are (d,q) components of rotor flux. The speed adaptive observer scheme with the speed adaptation mechanism is presented in Fig. 1.

4 Observer gain design

4.1 linearized model

The nonlinear and complicated dynamics of the speed adaptive observer can be studied via small-signal linearization. It is useful to proceed with a local analysis based in the principle of stability in the first approximation [12, 7].

We will choose the particular form $\underline{G}_1 = g_1 I_{2 \times 2}$ where $I_{2 \times 2}$ is the identity matrix and $\underline{G}_2 = 0_{2 \times 2}$. The complete adaptive observer may be written as equation (10). Note that according the assumption $\dot{\omega} = 0$, the motor model (1) may be written as (9)

$$\begin{cases} \frac{d}{dt}\underline{\psi}_r = -(\frac{1}{T_r} + j\omega_{sl})\underline{\psi}_r + \frac{L_m}{T_r}i_s \\ \frac{d}{dt}i_s = \frac{L_m}{b}(\frac{1}{T_r} - j\omega)\underline{\psi}_r - (a + j\omega_s)i_s + \frac{1}{\sigma L_s}u_s \\ \frac{d}{dt}\omega = 0 \end{cases} \quad (9)$$

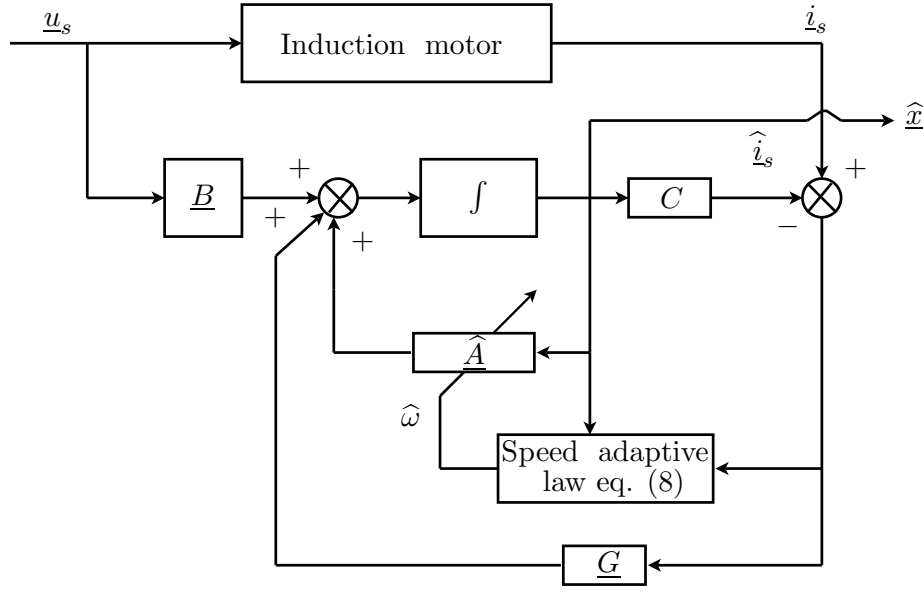


Figure 1: Speed adaptive observer

$$\begin{cases} \frac{d}{dt} \hat{\underline{\psi}}_r = -(\frac{1}{T_r} + j\hat{\omega}_s) \hat{\underline{\psi}}_r + \frac{L_m}{T_r} \hat{i}_s + g_1 \delta e_i \\ \frac{d}{dt} \hat{i}_s = \frac{L_m}{b} (\frac{1}{T_r} - j\hat{\omega}) \hat{\underline{\psi}}_r - (a + j\hat{\omega}_s) \hat{i}_s + \frac{1}{\sigma L_s} u_s \\ \frac{d}{dt} \hat{\omega} = K_p \frac{d}{dt} (e_{id} \hat{\underline{\psi}}_{rq} - e_{iq} \hat{\underline{\psi}}_{rd}) + K_i (e_{id} \hat{\underline{\psi}}_{rq} - e_{iq} \hat{\underline{\psi}}_{rd}) \end{cases} \quad (10)$$

We investigate the stability of the observer by linearizing the two systems (10) and (9) around an equilibrium operating point. Defining the new state vectors $\underline{x} = \underline{x}_o + \delta \underline{x}$ with $\underline{x}_o = [\underline{\psi}_{ro} \ i_{so} \ \omega_o]^T$, $\delta \underline{x} = [\delta \underline{\psi}_r \ \delta i_s \ \delta \omega]^T$ and $\hat{\underline{x}} = \hat{\underline{x}}_o + \delta \hat{\underline{x}}$ with $\hat{\underline{x}}_o = [\hat{\underline{\psi}}_{ro} \ \hat{i}_{so} \ \hat{\omega}_o]^T$, $\delta \hat{\underline{x}} = [\delta \hat{\underline{\psi}}_r \ \delta \hat{i}_s \ \delta \hat{\omega}]^T$. The reference frame is synchronized with the estimated rotor flux ($\hat{\underline{\psi}}_{rqo} = 0$), then its two components are $\hat{\underline{\psi}}_{rd} = \hat{\underline{\psi}}_o + \delta \hat{\underline{\psi}}_{rd}$ and $\hat{\underline{\psi}}_{rq} = \delta \hat{\underline{\psi}}_{rq}$. In these two systems, the stator frequencies are regarded as identical: $\omega_s = \hat{\omega}_s$ [5]. Preserving only dynamic parts, the two systems (9), (10) become after linearization,:

$$\begin{cases} \frac{d}{dt} \delta \underline{\psi}_r = -(\frac{1}{T_r} + j\omega_{slo}) \delta \underline{\psi}_r + \frac{L_m}{T_r} \delta i_s - j\hat{\Psi}_o \delta \omega_{sl} \\ \frac{d}{dt} \delta i_s = \frac{L_m}{b} (\frac{1}{T_r} - j\omega_o) \delta \underline{\psi}_r - (a + j\omega_{so}) \delta i_s + \frac{1}{\sigma L_s} \delta u_s - j\frac{L_m}{b} \hat{\psi}_o \delta \omega - j\hat{i}_{so} \delta \omega_s \\ \frac{d}{dt} \delta \omega = 0, \end{cases} \quad (11)$$

$$\begin{cases} \frac{d}{dt} \delta \hat{\underline{\psi}}_r = -(\frac{1}{T_r} + j\hat{\omega}_{slo}) \delta \hat{\underline{\psi}}_r + \frac{L_m}{T_r} \delta \hat{i}_s - j\hat{\Psi}_o \delta \hat{\omega}_{sl} + g_1 \delta e_i \\ \frac{d}{dt} \delta \hat{i}_s = \frac{L_m}{b} (\frac{1}{T_r} - j\hat{\omega}_o) \delta \hat{\underline{\psi}}_r - (a + j\hat{\omega}_{so}) \delta \hat{i}_s + \frac{1}{\sigma L_s} \delta u_s - j\frac{L_m}{b} \hat{\psi}_o \delta \hat{\omega} - j\hat{i}_{so} \delta \hat{\omega}_s \\ \frac{d}{dt} \delta \hat{\omega} = -K_p (-\frac{L_m}{b} \omega_o \hat{\psi}_o \delta \hat{\underline{\psi}}_{rd} + \frac{L_m}{b T_r} \hat{\psi}_o \delta \hat{\underline{\psi}}_{rq} - \omega_{so} \hat{\psi}_o \delta \hat{i}_{sd} - a \hat{\psi}_o \delta \hat{i}_{sq} - \frac{L_m}{b} \hat{\psi}_o \delta \hat{\omega}_s) \\ \quad - K_i (-e_{ido} \delta \hat{\underline{\psi}}_{rq} + e_{iqo} \delta \hat{\underline{\psi}}_{rd} + \hat{\underline{\psi}}_o \delta e_{iq}). \end{cases} \quad (12)$$

Defining $\delta \underline{e} = [\delta e_\psi \quad \delta e_i \quad \delta e_\omega]^T$, the system describing the estimation error is as follows:

$$\begin{cases} \frac{d}{dt} \delta e_\psi = -\left(\frac{1}{T_r} + j\omega_{slo}\right) \delta e_\psi + \left(\frac{L_m}{T_r} - g_1\right) \delta e_i - j e_{\psi_o} \delta \omega_{sl} + j e_{\omega_o} \delta \hat{\psi}_r + j \hat{\psi}_o \delta e_\omega \\ \frac{d}{dt} \delta e_i = \frac{L_m}{b} \left(\frac{1}{T_r} - j\omega_o\right) \delta e_\psi - (a + j\omega_{so}) \delta e_i - j \frac{L_m}{b} e_{\psi_o} \delta \omega - j \frac{L_m}{b} e_{\omega_o} \delta \hat{\psi}_r \\ \quad - j e_{io} \delta \omega_s - j \frac{L_m}{b} \hat{\psi}_o \delta e_\omega \\ \frac{d}{dt} \delta e_\omega = K_p \left(-\frac{L_m}{b} \omega_o \hat{\psi}_o \delta e_{\psi d} + \frac{L_m}{b T_r} \hat{\psi}_o \delta e_{\psi q} - \omega_{so} \hat{\psi}_o \delta e_{id} - a \hat{\psi}_o \delta e_{iq} - \frac{L_m}{b} \hat{\psi}_o \delta e_\omega\right) \\ \quad + K_i (-e_{ido} \delta \hat{\psi}_{rq} + e_{iqo} \delta \hat{\psi}_{rd} + \hat{\psi}_o \delta e_{iq}). \end{cases} \quad (13)$$

Separating each state in d and q components, we obtain the corresponding state matrix \hat{A}_1 :

$$\hat{A}_1 = \begin{bmatrix} -\frac{1}{T_r} & \omega_{slo} & \frac{L_m}{T_r} - g_1 & 0 & 0 \\ -\omega_{slo} & -\frac{1}{T_r} & 0 & \frac{L_m}{T_r} - g_1 & \hat{\psi}_o \\ \frac{L_m}{b T_r} & \frac{L_m}{b} \omega_o & -a & \omega_{so} & 0 \\ -\frac{L_m}{b} \omega_o & \frac{L_m}{b T_r} & -\omega_{so} & -a & -\frac{L_m}{b} \hat{\psi}_o \\ -\frac{L_m}{b} K_p \omega_o \hat{\psi}_o & \frac{L_m}{b T_r} K_p \hat{\psi}_o & -K_p \omega_{so} \hat{\psi}_o & (K_i - a K_p) \hat{\psi}_o & -\frac{L_m}{b} K_p \hat{\psi}_o \end{bmatrix} \quad (14)$$

Note the dependency of the dynamic matrix \hat{A}_1 by the operating condition. In order to obtain analytic conditions about the local stability using the necessary condition for stability based on the determinant of (14) [4], it is possible to obtain a relevant result as reported in the next section.

4.2 Stability criterion

We use the following property:

$$\det(\hat{A}_1) = \prod_{i=1}^5 \lambda_i \quad (15)$$

where λ_i are the eigenvalues of matrix \hat{A}_1 .

The determinant of matrix \hat{A}_1 is:

$$\det(\hat{A}_1) = -L_m \hat{\psi}_o^2 K_i \omega_{so} ((\omega_{so} - \omega_o) a b T_r + L_m^2 \omega_o - L_m \omega_o g_1 T_r + \omega_{so} b) / (b^2 T_r) \quad (16)$$

The condition $\det(\hat{A}) = 0$ leads to:

$$\omega_{so} = 0, \quad (17a)$$

$$\omega_{so} = \omega_o \frac{g_1 L_m + R_s L_r}{(R_r L_s + R_s L_r)}. \quad (17b)$$

These conditions of stability may be expressed in the torque/speed plane. Let us consider the mechanical equation:

$$\frac{d}{dt} \omega = p^2 \frac{L_m}{J L_r} \Im(i_s \underline{\psi}_r^*) - p \frac{T_L}{J}. \quad (18)$$

Under RFOC conditions and steady state ($\hat{\psi}_{rqo} = \psi_{rqo} = 0$), we obtain:

$$0 = p \frac{L_m}{L_r} \hat{\psi}_o i_{sqo} - T_{Lo} \quad (19)$$

then

$$i_{sqo} = \frac{L_r}{pL_m\hat{\psi}_o} T_{Lo}. \quad (20)$$

From system (1), in the same conditions, we find :

$$\omega_{slo} = \frac{L_m}{T_r\hat{\psi}_o} i_{sqo}. \quad (21)$$

Finally using $\omega_{so} = \omega_{slo} + \omega_o$, equations (17a) and (17b) become

$$T_{Lo} = -\frac{p\hat{\psi}_o^2}{R_r} \omega_o \quad (22a)$$

$$T_{Lo} = -\frac{p\hat{\psi}_o^2}{R_r} \frac{(1 - \frac{g_1 L_m}{R_r L_s}) \omega_o}{(1 + \frac{T_s}{T_r})} \quad (22b)$$

with $T_s = L_s/R_s$. Above relations describe respectively two lines, defining two well known instability regions in regenerating mode.

An sufficient condition for instability is then:

$$\det(\hat{A}_1) > 0. \quad (23)$$

The condition (23) defines a set whose the instability region is a subset. In order to complete the study of local stability, we plot for each eigenvalue, the locus in the torque/plane where conditions $(\Re(\lambda_i) > 0, i = 1 \dots 5)$ are verified.

In one hand, if we chose a zero observer gain, as in [9],

$$g_1 = 0 \quad (24)$$

we obtain the instability region limited by lines D_1 and D_2 , (Fig. 1) where $\Re\lambda_i > 0, i = 1 \dots 5$, are the positive real part of the eigenvalues λ_i of the state matrix \hat{A}_1 . The eigenvalues correspond respectively to the states variables $\delta e_{\psi_{rd}}, \delta e_{\psi_{rq}}, \delta e_{id}, \delta e_{iq}$ and δe_{ω} .

$$T_{Lo} = -\frac{p\hat{\psi}_o^2}{R_r} \frac{\omega_o}{(1 + \frac{T_s}{T_r})} \quad (25)$$

In other hand, in order to reduce (not totally remove) the unstable region, a real valued observer gain was considered in [13] which corresponds to the region limited by lines D_1 and D_3 , (Fig. 3). The value of the parameter g_1 selected is:

$$g_1 = -0.25R_s \quad (26)$$

It is be noted that the curves corresponding to zero observer gain are similar, except that the unstable region is larger.

$$T_{Lo} = -\frac{p\hat{\psi}_o^2}{R_r} \frac{(1 + \frac{0.25R_s L_m}{R_r L_s}) \omega_o}{(1 + \frac{T_s}{T_r})} \quad (27)$$

The principle of the instability reduction proposed here consists in the calculation of the feedback gain so that the unstable region will be limited to the inobservability line (D_1). We can note that, whatever the structure of the matrix G , (D_1) is always defined by $\omega_{so} = 0$. From equation (16), we can write the

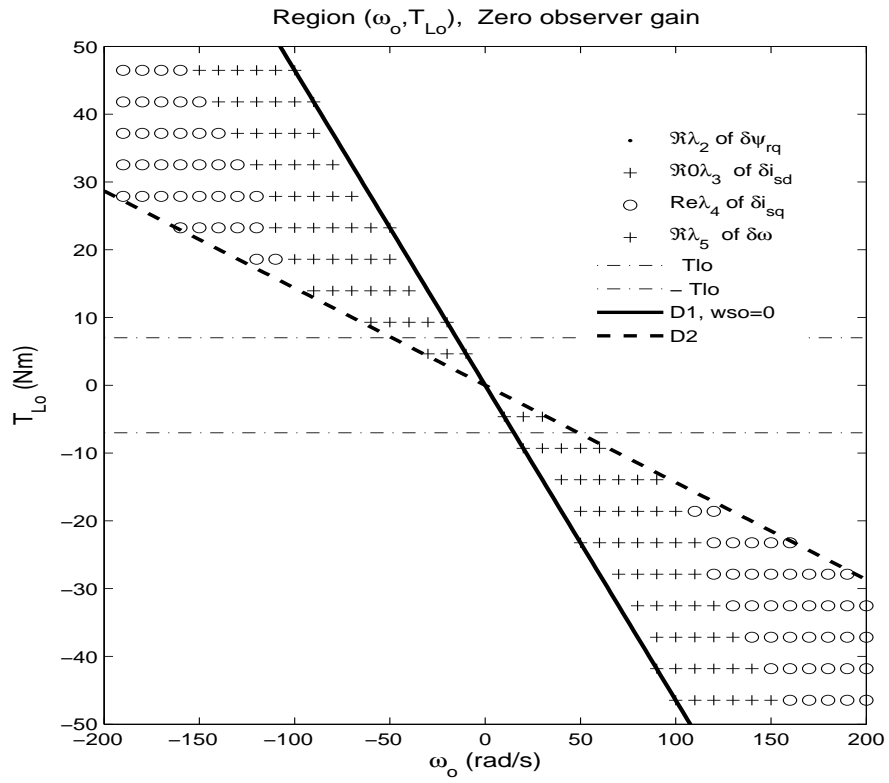


Figure 2: Torque/speed plane, $g_1 = 0$, $\Re(\lambda_i) > 0, i = 1 \dots 5$

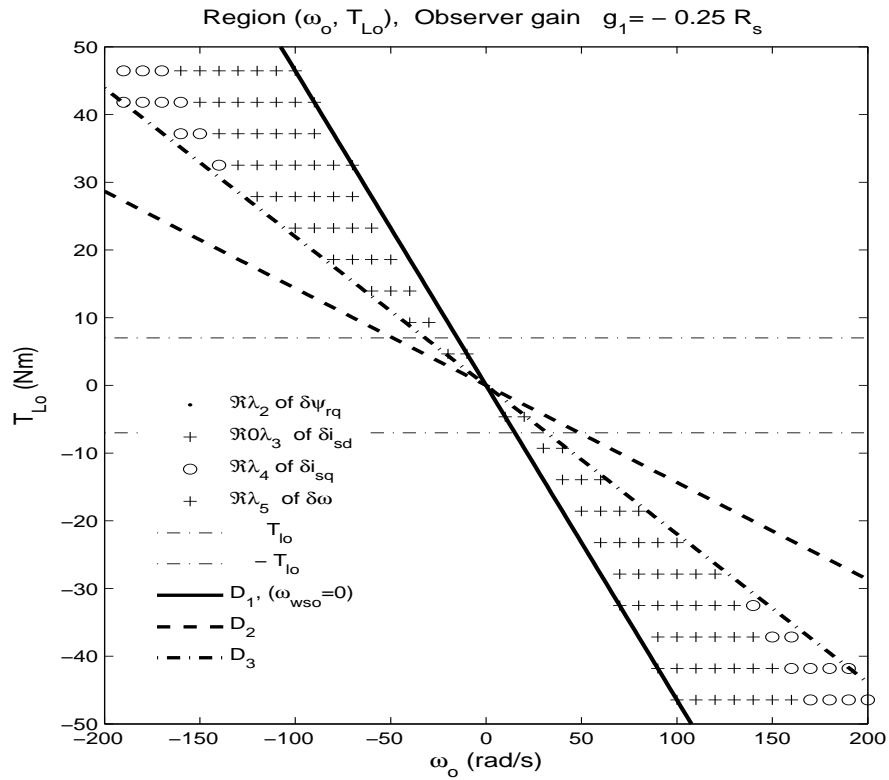


Figure 3: Torque/speed plane, $g_1 = -0.25 R_s$, $\Re(\lambda_i) > 0, i = 1 \dots 5$

condition $\omega_{so} = 0$ in equation (28)

$$(\omega_{so} - \omega_o)abT_r + L_m^2\omega_o - L_m\omega_o g_1 T_r + \omega_{so}b = 0 \quad (28)$$

which can be achieved by choosing the following observer gains

$$g_1 = -\frac{L_r R_s}{L_m} \quad (29)$$

The straight line (D_1) correspond to zero synchronous speed $\omega_s = 0$. It is known in the literature as the inobservability line (normally referred as dc-excitation) [6, 3] and seems to be a generic problem for sensorless control of induction motors.

5 Simulations results

In order to validate the proposed design, the regenerating mode low speed operation of the speed adaptive observer was investigate by means of simulations. A rotor flux oriented control (RFOC) is simulated using Matlab/Simulink software. The block diagram of the control system is shown in Fig.4. The flux reference is fixed to the nominal value ψ_o^{ref} where ref denotes the reference value. The proposed

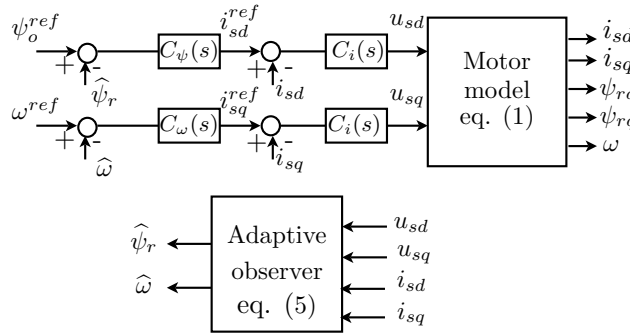


Figure 4: Block diagram of sensorless RFOC induction motor simulator.

observer is compared with an exiting solution [13]. In order to validate the proposed design, we studied a conventional test used by industrial drive designers: very low and progressive load torque increase under constant speed; Fig. 5 depicts results in regenerating mode obtained using the observer gain $g_1 = -0.25R_s$, [13], [5]. The speed reference was set to $(-25rad/s)$ (dashed line) and a rated-load torque ramp was applied at $t=0$. After applying the load progressively, the drive should operate in the regenerating mode. However, the actual angular speed et actual flux of the motor collapse and the system becomes unstable. Fig. 6 present results obtained using the proposed observer design. The system behaves stably. On Fig. 7, the observer gain $g_1 = -0.25R_s$ was used. Real speed diverges. First subplot shows reference (dashed line) and actual angular speed. Second subplot shows rated-load torque ramp. Third subplot present actual flux components ($\psi_{r\alpha}, \psi_{r\beta}$) in stator reference frame. Fouth subplot, shows control voltages. In the fifth and six subplot respectively, we present current and current norm. We note that when the load torque increases, the control voltage, the current and the current norm increase too. On Fig.8, the proposed observer design was used. The system becomes stable. Real rotor angular speed converges well towards the reference value in response to the same rated-load torque. Note the behavior of the actual flux at $(t \approx 3.75 s)$ when the real angular rotor speed crosses the line ($D_1 = D_3$). The system becomes unobservable at this time.

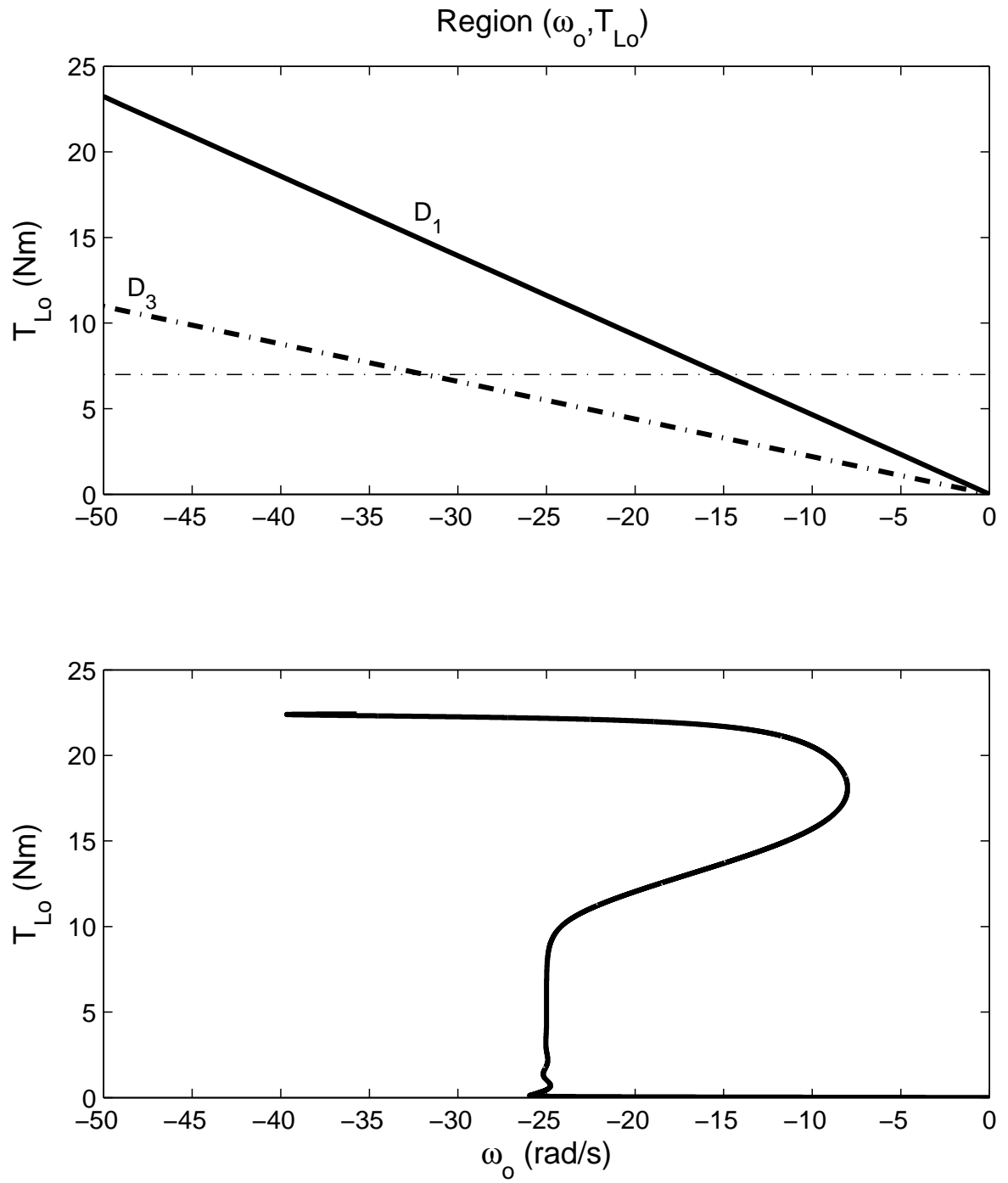


Figure 5: A rated-load torque ramp is applied with the observer gain $g_1 = -0.25R_s$. First subplot shows region (ω_o, T_{Lo}) with the two lines D_1 and D_3 . Second subplot shows the actual angular speed.

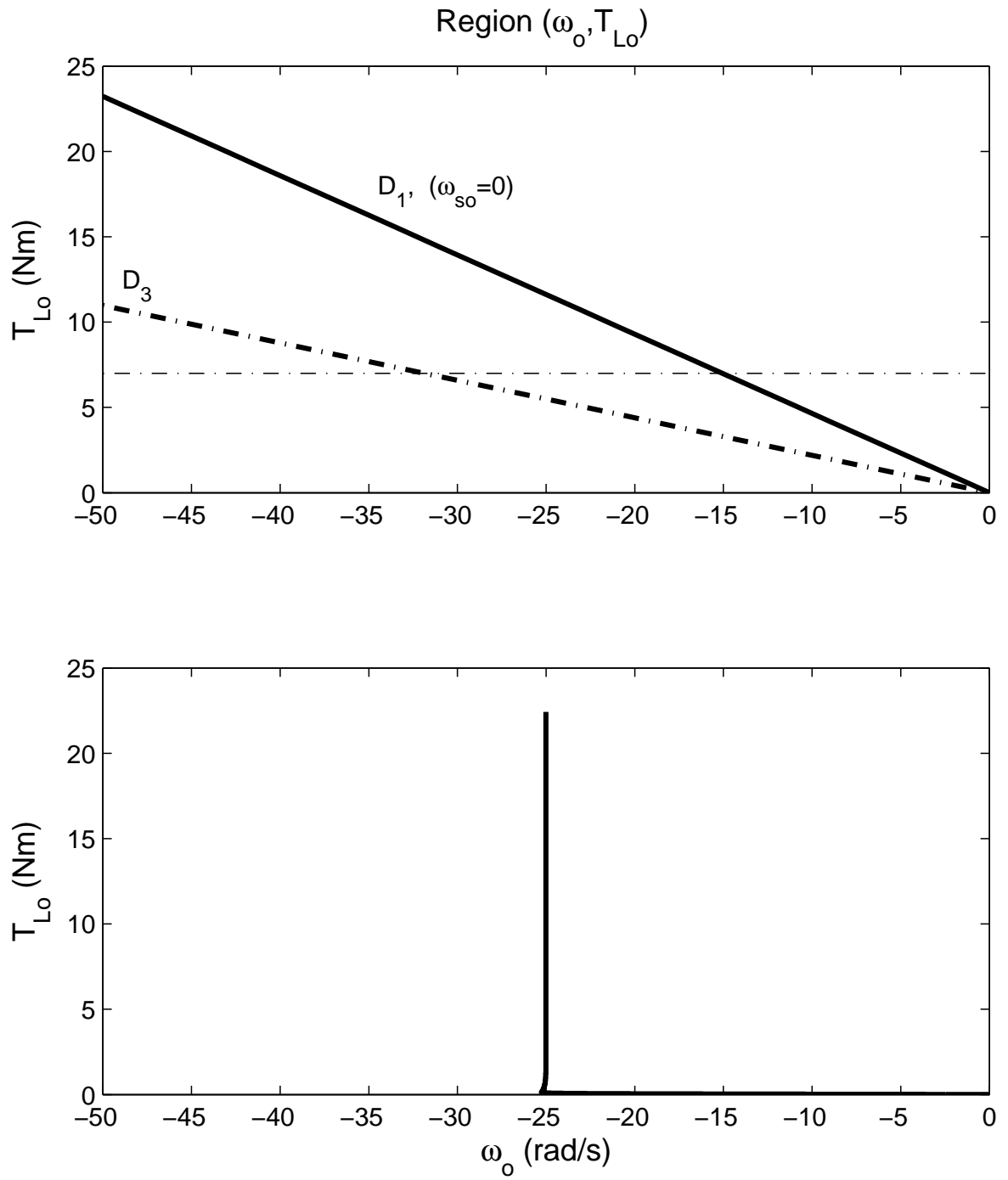


Figure 6: A proposed observer design was used. First subplot shows region (ω_o, T_{Lo}) with the line $D_1 = D_3$. Second subplot shows the actual angular speed.

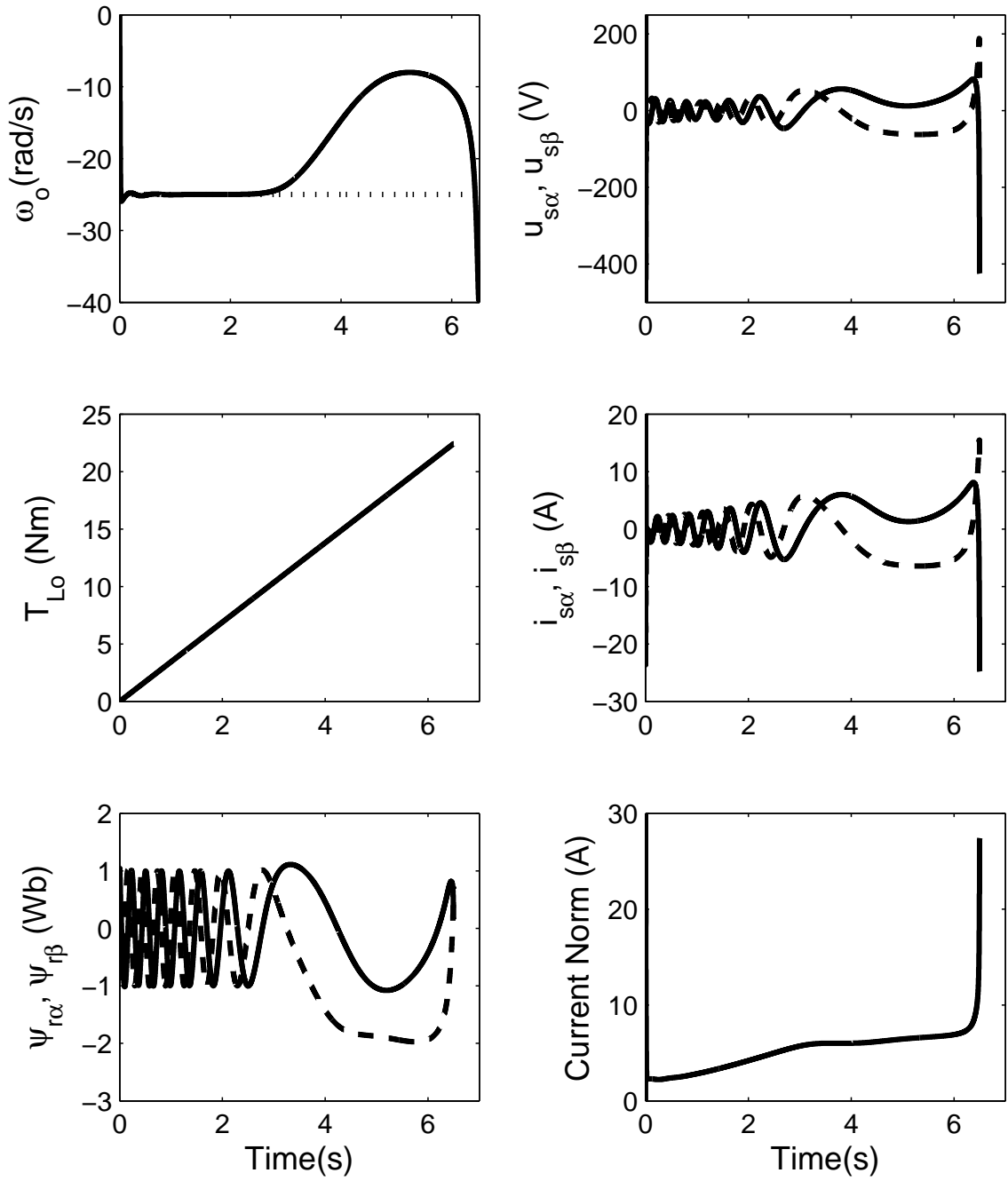


Figure 7: Instability phenomenon with observer gain $g_1 = -0.25R_s$.

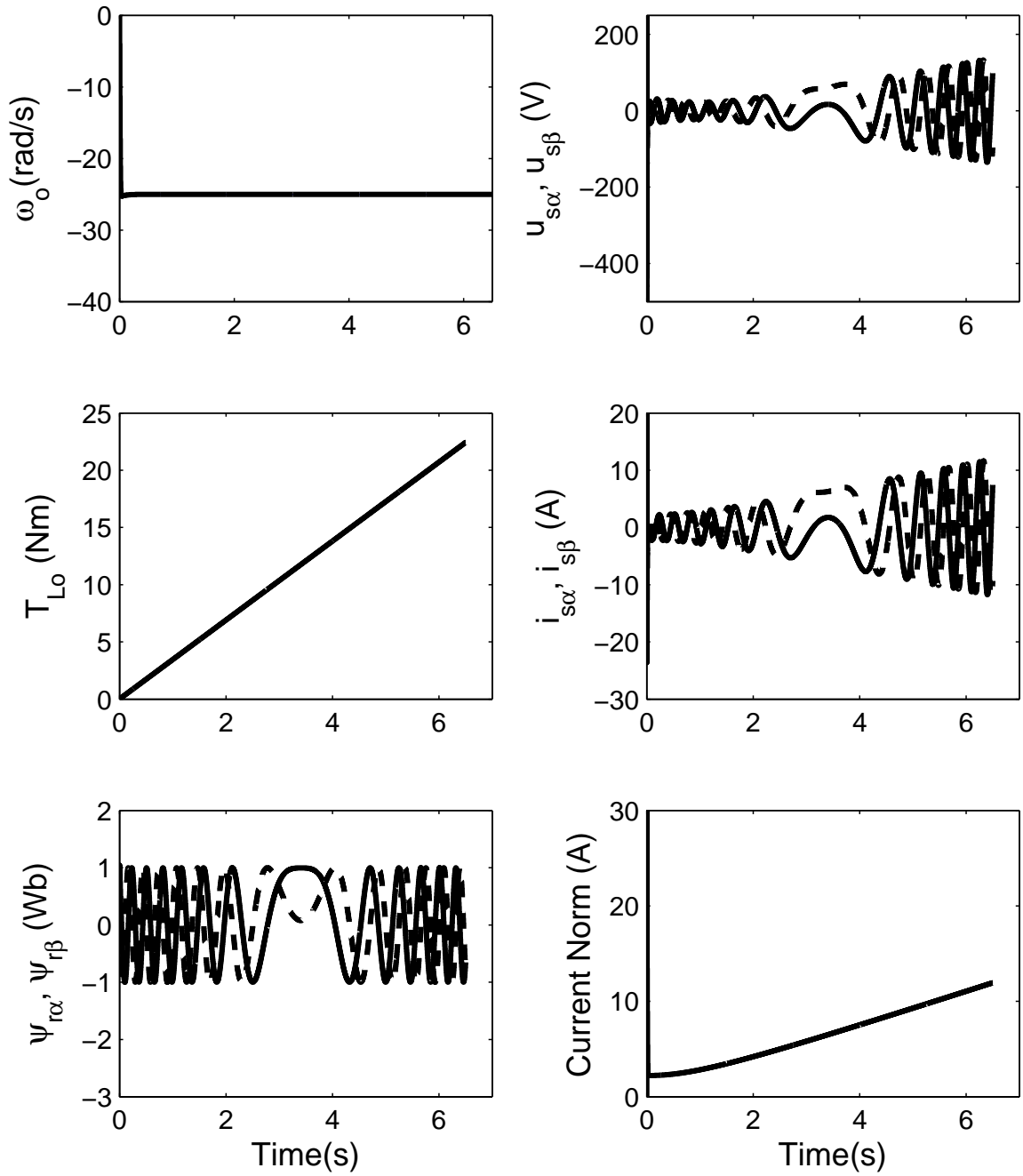


Figure 8: The instability was removed by the proposed observer design $g_1 = -L_r R_s / L_m$.

6 Appendix

6.1 Induction motor parameters

Voltage rating : 380 V, Current rating: 2.2 A, Number of phases: 3, Rated power: 1.1 kW, Frequency: 50 Hz, Rated speed: 1430 rpm/min, $p = 2$, $L_s = 0.472$ H, $L_r = 0.4721$ H, $L_m = 0.4475$ H, $R_s = 9.65$ Ω , $R_r = 4.3$ Ω .

7 Conclusions

The feedback gain design method proposed in this paper reduces the instability region of adaptive observer to a inobservability line (D_1) ($\omega_{so} = 0$). The observer using the proposed gain does not have the unstable region, which was shown by means of speed/torque plane and a linearized model. The stability of the regenerating-mode operation was also confirmed by simulations.

Bibliography

- [1] A. Bouhenna, C. Chaigne, N. Bensiali, E. Etien and G. Champenois, Design of speed adaptation law in sensorless control of induction motor in regenerating mode, *Simulat. Modell. Pract. Theory, Elsevier*, doi:10.1016, simpat.2007.04.005, Vol. 15, No.7, pp. 847-863, 2007.
- [2] A. Bouhenna, Contribution à la commande sans capteur mécanique de la machine asynchrone en mode générateur à basse vitesse, *Thèse de Doctorat en Sciences, Université des Sciences et de la Technologie d'Oran, Algérie*, octobre, 2007.
- [3] C. Canudas De Wit and A. Youssef and J. P. Barbot and PH. Martin and F. Malrait, Observability Conditions Of Induction Motors At Low Frequencies, *Proc. CDC, Sydney*, pp. 1-7, 2000.
- [4] E. Etien and N. Bensiali and C. Chaine and G. Champenois, Adaptive Speed Observers For Sensorless Control Of Induction Motors: A New Criterion Of Stability, *International review of electrical engineering*, Vol. 1, pp. 36-43, 2006.
- [5] M. Hinkanen, Stabilization Of Regenerating-Mode Operation in Sensorless Induction Motor Drives By Full-Order Flux Observer Design, *IEEE Trans. Ind. Electron.*, Vol. 51, pp. 1318-1328, 2004.
- [6] H. Hofmann and S. Sanders, Speed-Sensorless Vector Torque Control Of Induction Machine Using A Two-Time-Scale Approach, *IEEE Trans. on Ind. Appl.*, Vol. 34, pp. 169-177, 1998.
- [7] H. K. Khalil, *Nonlinear systems*, Macmillan, New York, 1983.
- [8] H. Kubota and K. Matsuse, DSP-Based Speed Adaptive Flux Observer Of Induction Motor, *IEEE Trans. Ind. Appl.*, Vol. 29, pp. 344-348, 1993.
- [9] H. Kubota and I. Sato, Regenerating Mode Low Speed Operation Of Sensorless Induction Motor Drive With Adaptive Observer, *IEEE Trans. Ind. Appl.*, Vol. 38, pp. 1081-1086, 2002.
- [10] A. Mansouri and M. Chenafa and A. Bouhenna and E. Etien, Powerful nonlinear observer associated with field-oriented control of an induction motor, *International Journal of Applied Mathematics and Computer Sciences*, Vol. 14, No. 2, pp. 209-220, 2004.

- [11] M. Chenafa and A. Mansouri and A. Bouhenna and E. Etien and A. Belaidi and M. A. Denai, Global stability of linearizing control with a new robust nonlinear observer of the induction motor, *International Journal of Applied Mathematics and Computer Sciences*, Vol. 15, No. 2, pp. 235-243, 2005.
- [12] M. Montanarri and S. Peresada and A. Tilli, Observeless Scheme For Sensorless Control Of Induction Motor: Stability Analysis And Design Procedure, *Proc. of the 10th Mediterranean Conference and Automation, Med'02, Lisbon, 2002*.
- [13] S. Suwankawin and S. Sangwongwanich, Speeds Sensorless IM Drive With Decoupling Control And Stability Analysis Of Speed Estimation, *IEEE Trans. Ind. Electron.*, Vol. 49, pp. 444-455, 2002.
- [14] S. Suwankawin and S. Sangwongwanich, Design strategy of an adaptive full order observer for speed sensorless induction motor drives-tracking performance and stabilization, *IEEE Trans. Ind. Electron.* Vol. 53, pp. 96-119, 2006.
- [15] G. Yang and T. Chin, Adaptive-Speed Identification Scheme For A Vector-Controlled Speed Sensorless Inverter-Induction Motor Drive, *IEEE Trans. Ind. Appl. Electron.*, Vol. 29, pp. 820-825, 1993.

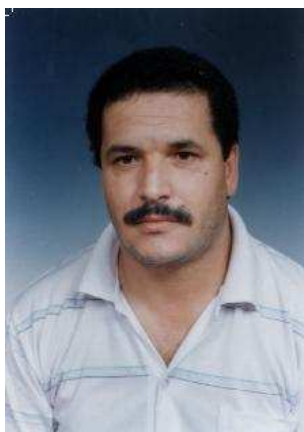
A. Bouhenna¹, A. Mansouri¹, M. Chenafa¹, and A. Belaidi¹

¹ E.N.S.E.T. d'Oran, Laboratoire d'Automatique et d'Analyses des Systèmes, (L.A.A.S) Département de Génie électrique, B.P 1523, El M'naouer, Oran, Algérie
E-mail: bouhenna @ enset-oran.dz, (abouhenna @ yahoo.fr)

Received: October 10, 2007.



Abderrahmane BOUHENNA was born in 1955. He received the Dipl. Eng. degree in electronic engineering, the M. S degree and the Doctorat in automatic from U.S.T.O, Oran, Algeria in 1980, 1987 and 2007 respectively. He is currently a professeur searcher in the laboratory of automatic and analysis systems at ENSET of Oran (Algeria). He work on the subject of sensorless control and observers of induction motors and obtained some results in this domain for the stabilisation of the observers and the control of the MAS in regenerating mode at low speed.



Abdellah MANSOURI was born in Oran in Algeria, in 1953. He received his BS degree in electronic engineering from USTO (Algeria) in 1979, the MS degree in engineering control from USTO (Algeria) in 1991, and the PhD degree in engineering control from USTO (Algeria) in 2004. He is currently professor of automatic control at ENSET of Oran (Algeria). His research interests are non linear control and observers applied in induction motor and manipulator robot.



Mohammed CHENAFI was born in Oran in Algeria, in 1954. He received his BS degree in electronic engineering from USTO (Algeria) in 1979, the MS degree in signal processing and robotic from USTO (Algeria) in 1998, and the PhD degree in engineering control from USTO (Algeria) in 2005. He is currently professor of automatic control at ENSET of Oran (Algeria). His research interests are non linear control and observers applied in induction motor and manipulator robot.



Abdelkader BELAIDI, Professor In 1981 he obtained a Ph.D in radiation Physics at the University of East Anglia, Norwich - England. His fields of interest are collision damage in materials and neural and fuzzy logic. Now, he is a professor of physics and applied computing at the Higher School of Education - Oran Algeria. He is also head of Automatic and System Analysis Laboratory (LAAS).